

Utilizing Absorbed Heat from Concrete to Generate Clean Electricity

by

Haroon Ehsan, Kate Caulfield and Yenthy Luong

Governor School at Innovation Park

COS120: Introduction to Research

Dr. Ales Psaker

January 6, 2026

Acknowledgments

Our group of Haroon, Kate, and Yenthy would like to acknowledge our support and resources granted by our mentor, Dr. Ales Psaker. We'd also like to thank the Governor School at Innovation Park for facilitating an environment where we are enabled to practice this research in the George Mason Science and Technology Campus.

Abstract

A phenomenon known as the Urban Heat Island (UHI) affects when surrounding infrastructure absorbs thermal energy and radiates heat slowly into the environment, wasting thermal energy and causing negative health effects. An attribute of conductors (or semiconductors) is when there is a temperature difference within a semiconductor, a voltage is created. This phenomenon is known as the Seebeck effect which can be measured with the Seebeck coefficient. This means that we can transform the heat into electricity. Our team plans to mitigate the UHI effect and utilize the thermal properties of concrete to generate electricity in the most cost-effective way. This would benefit areas which don't have much funds yet still want to reduce UHI. Our plan is to compare Seebeck coefficient when different fillers are added to concrete. We plan to do this by mixing up cement samples with fillers, cure them into concrete cubes, insulate it while heating one side and cooling the other, measure the temperature and voltage difference along with current and resistance to get the Seebeck coefficient. At the moment our team hasn't carried out this experiment and don't have our own results, however for the past few months we have researched various articles regarding Cement-Based Thermoelectric Material (CTEM) providing us with useful data for this research. We plan to test various filler types (Carbon Filler, Fe_2O_3 , Graphite powder and fly ash), which fly ash and Carbon fillers (CF) have found to have the largest Seebeck coefficient when utilized together. Fly ash on its own is only able to produce $-15 \mu\text{V/K}$ (Cao et al. 2020) yet when mixed with CF, it is able to produce results ranging from $866 \mu\text{V/K}$ (Paio et al. 2025), $1123 \mu\text{V/K}$ (Wan et al. 2018) and $6000 \mu\text{V/K}$ (Ran et. al, 2024).

Chapter 1 - Introduction

Concrete is one of the most widely used construction materials in the world, forming the foundation of modern infrastructure. However, its widespread use significantly contributes to global warming and imbalances in urban temperatures. Large expanses of concrete and asphalt absorb substantial amounts of solar radiation during daylight hours and release the heat back into the atmosphere slowly, intensifying a phenomenon known as the Urban Heat Island (UHI) effect. The UHI effect describes the tendency for urban areas to experience significantly higher temperatures than surrounding rural regions due to dense concentrations of man-made structures that reflect heat poorly, have low amounts of vegetation, and are made of materials that absorb much more heat compared to natural ground (Zafra, 2025). Concrete has a high thermal mass, meaning it's great at storing and absorbing heat (Reardon, 2020). According to the US EPA (2024), urban temperatures can be 1-7° C higher than nearby rural areas during the day.

The UHI effect has become increasingly concerning in the context of climate change. Tong et al. (2021) report that the urban heat island effect can have severe effects on not only the climate, but the populations of cities themselves. These elevated urban temperatures have been shown to cause significant mortalities, seriously affecting elderly and low-income people. Additionally, it increases energy demands for cooling and can strain power grids during times of high demand. This heat, while harmful, can be utilized in a more productive way, and is a vastly underutilized energy source. Rather than being put to use, most of this thermal energy is simply re-emitted into the atmosphere.

One strategy to address both waste heat and sustainability challenges is the use of thermoelectric materials, which can directly convert heat into electricity. Thermoelectric energy conversion is governed by the Seebeck effect, a phenomenon in which a temperature difference across a conductive or semiconductive material generates an electric voltage (Li et al., 2025). When there is a temperature difference across a thermoelectric material, charge carriers migrate from the hot to the cold side,

producing an electric potential difference. This process allows thermal energy to be converted directly into electrical energy with zero moving parts (Jaziri et al., 2019).

Thermoelectric devices are especially attractive for waste-heat recovery applications because they are long-lasting, require minimal maintenance, and able to function in harsh environments. Singh et al. (2021) emphasize that thermoelectric generators (TEGs) are among the most practical energy-harvesting technologies due to their lack of moving parts and lack of carbon emissions. These advantages have enabled thermoelectric devices to be successfully deployed in extreme conditions where conventional power generation is impractical. One notable example of such qualities in TEGs is its use in the Voyager spacecrafts (NASA, 2023).

Building on this proven technology, lots of recent research has focused on developing cement-based thermoelectric materials (CTEMs) by incorporating conductive or semiconductive fillers into traditional cement matrices. Materials such as carbon fibers, graphite, metal oxides, and industrial waste can introduce charge-carrier pathways within concrete, allowing infrastructure itself to function as a thermoelectric generator. By harvesting temperature gradients naturally present in urban environments, such as those between sun-exposed surfaces and cooler subsurface regions, CTEMs offer the potential to simultaneously mitigate UHI effects and generate clean renewable energy.

Question

Within this research, we plan to investigate which fillers in cement provide the highest Seebeck coefficient (S) and figure of merit (ZT) while staying affordable and practical.

Hypothesis

We predict that the cement fillers will increase the Seebeck Coefficient and generate thermoelectricity due to its conductive properties.

We expect hybrid mixtures of Fly Ash, Graphite Powder, and Carbon Fiber (CF), as well as mixtures of Fe_2O_3 and CF to be most effective.

The Null Hypothesis states that the inclusion of fillers will not have any meaningful effect on the Seebeck coefficient of the cement samples.

Chapter 2 – Materials and Methods

The materials we will use during this experiment are: Portland Cement Mix, Water, Superplasticizer, Graphite Powder, Fly ash, Fe_2O_3 , Carbon Fiber (CF), Cement dye, 2 K-type Thermocouples, 2 Multimeters, Copper plates, a 50 W Heat Lamp and Foam Core Insulator Roll.

Our experiment involves heating up samples of modified cement and measuring the produced voltage. To produce the cement samples needed, we will mix 4-inch cubic cement samples containing the fillers, along with superplasticizer to increase particle dispersion and black cement dye to increase heat absorption. One control sample with no additive will also be produced. Since moisture has a significant effect on the thermoelectric properties of CTEMs (Wei et al., 2017), each sample will be cured and dried completely. We will include samples containing fly ash, graphite powder, Fe_2O_3 , CF, and mixtures of these fillers at varying percent weights.

The apparatus in which the experiment will be conducted will be similar to the ones shown in the 2 figures below. The sample will be placed between two electrodes on opposite faces, one hot and one cold. The cold electrode will be connected to water, and the hot insulator will be exposed to a work lamp to simulate heat from sunlight. To prevent leakage of temperature outside the sample, it will be wrapped in insulation. Each electrode will have a thermocouple to collect temperature values at each end, along with copper sheets connected to a multimeter to measure voltage. Measurements of temperature difference (ΔT) and Voltage difference (ΔV) at multiple points in time will be taken and divided to find Seebeck Coefficient (S).

In addition to finding the Seebeck coefficient, additional data regarding the electrical and thermal properties of the sample will also be collected. A known current will be passed through the electrodes of the cement sample. Using the four-probe method, another multimeter will be between the two current probes to measure voltage. Using Ohm's law ($R = V/I$), we can then use the current and voltage to get the resistance.

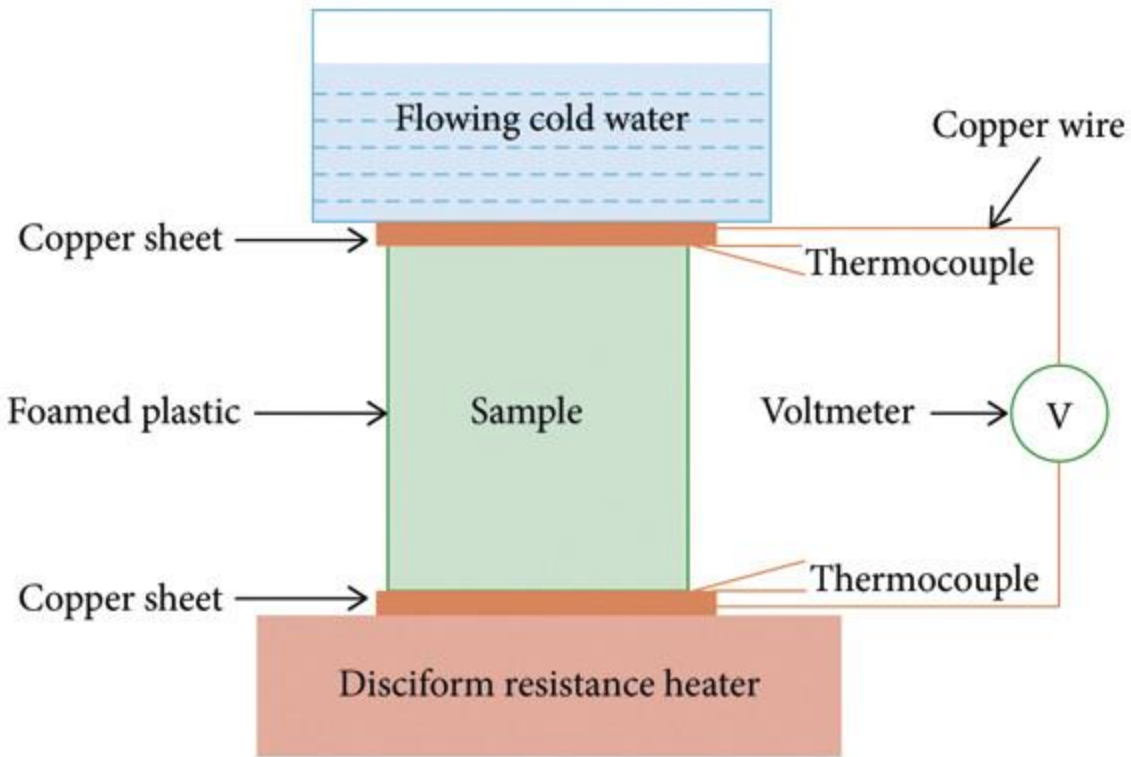


Figure 1. A diagram picturing a method to determine the Seebeck Coefficient of a sample (Ji et al., 2022)

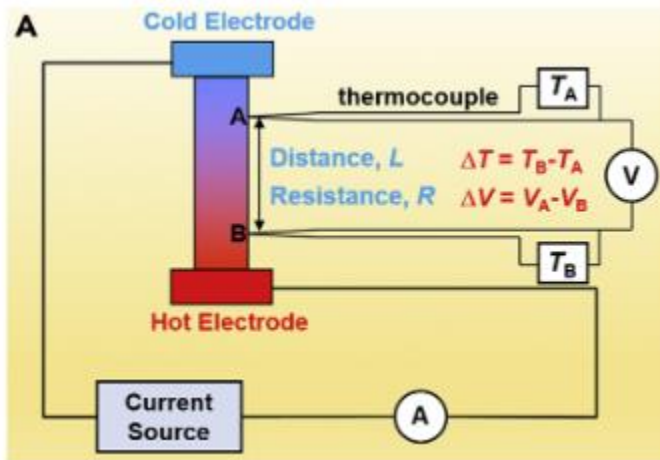


Figure 2. Schematic of S and σ measurements from (Wei et al., 2018)

Chapter 3 – Data Analysis

The data values we have collected from the experiment are Temperature Difference (ΔT), Voltage Difference (ΔV), Supplied Current (I), and Voltage from the current (U). Additionally, the dimensions of the cement sample (4" x 4" x 4") and percent-volume of each filler will also be recorded for each trial. The main tool for data visualization and analysis we will be using will be MATLAB.

There will be many values for ΔT and ΔV in each trial. ΔV will be plotted vs ΔT , and the slope between the two will be calculated to find Seebeck coefficient S ($\mu\text{V/K}$). Regarding the second experiment for each sample, in which electrical properties are measured, we will need to calculate the electrical conductivity (σ), thermal conductivity (κ), and figure of merit ZT.

First, to calculate the electrical conductivity, we use Ohm's law ($V=IR$) to find the resistance (R) in the cement sample. We then find electrical resistivity (ρ) with the equation $\rho = \frac{R \cdot A}{L}$, with A being cross-sectional area and L being length of the sample. In the case of our experiment, all dimensions of the sample are 4" (10.16 cm). Electrical conductivity σ is calculated as $\sigma = \frac{1}{\rho}$. We will be using the same equation as used by Ji et al. (2022) to find thermal conductivity $\kappa = \frac{I \cdot U \cdot L}{S \cdot \Delta T}$. Finally, the figure of merit can be found as $ZT = \frac{S^2 \cdot T \cdot \sigma}{\kappa}$, where T is absolute temperature (Li et al., 2025).

Chapter 4 – Results/Discussion

As we have not conducted our experiment yet, we do not have any results of our own. However, we have conducted an extensive literature review regarding recent advances in CTEM technology. Of our three chosen filler types (CF, Fe_2O_3 , Graphite powder, and Fly ash), fly ash and CF have shown to provide the best Seebeck coefficient. CTEMs enhanced with fly ash and CF have produced S values of around 6000 $\mu\text{V/K}$ (Ran et al., 2024). Cao et al. (2020), however, found that fly ash alone was only capable of producing S values of up to $-15 \mu\text{V/K}$. Piao et al. (2025) found that incorporation of CF could provide a S

value of up to 866 $\mu\text{V/K}$ at 0.3 percent weight. Wan et al. (2018) found that $\text{Fe}_2\text{O}_3 + \text{CF}$ could produce S values of up to 1123 $\mu\text{V/K}$.

We find that CF is the most effective filler, but only when hybridized with other fillers, as its results alone are lackluster. Iron Oxide, due to its semiconductive nature, can provide high Seebeck coefficients by itself and perform even better when hybridized with other fillers. Fly ash, while its thermoelectrically enhancing effects are minimal, plays a key contribution in modifying the microstructure and properties of the cement itself. Its influence on ionic conduction and thermal conductivity boosts other fillers. Outside of CTEMs, fly ash is also commonly used in cement for sustainability, durability, and cost reduction. Graphite powder is low-cost and is known for its electrical conductivity. Compared to CF, graphite typically provides more conductivity but with less mechanical reinforcement. While the thermoelectric properties of graphite may not be as great as Fe_2O_3 or CF, it has shown to enhance the properties of CF (Cao et al., 2010).

Table 1. Depicted is a table from Ran et al. (2024) comparing the efficiency of Carbon Fibers (CF) and its thermoelectric performance.

Materials	S	σ	PF	K	ZT	Ref
Control	3224.27	4.5×10^{-4}	4.68×10^{-3}	0.59	2.47×10^{-6} (40°C)	This study (Saturated)
M-0.5-9	5899.62	4.03×10^{-4}	1.4×10^{-2}	0.62	7.03×10^{-6} (40°C)	
M-1.0-15	5932.16	4.83×10^{-4}	1.7×10^{-2}	0.58	9.17×10^{-6} (40°C)	
M-1.0-6	3237.34	0.00234	2.45×10^{-2}	0.59	1.3×10^{-5} (40°C)	
CF (1.0wt%)+ Fe ₂ O ₃ (5.0wt%)	154.7– 386.8	$0.5–1 \times 10^{-2}$ 2	2.08	0.22	3.11×10^{-3}	[26]
CF+Fe ₂ O ₃ (5.0wt%)	1123.4	–	–	–	8.51×10^{-5} (85°C)	[35]
Graphite/CF	1.25	78	7.85×10^{-4}	–	–	[33]
CF (1.0wt%)	22.07	0.20008	–	0.22	0.33×10^{-7} (20°C)	[20]
CF+5.0wt% Fe ₂ O ₃	92.57	–	–	–	–	[36]
CF+5.0wt% Bi ₂ O ₃	100.28	–	–	–	–	
MWCNT (0.140vol%)	13.67	2.52×10^{-2}	4.71×10^{-6}	1.89	7.48×10^{-10}	[44]
MWCNT (15.0wt%)	53	81.8	2.3×10^{-1}	0.95	7.27×10^{-5}	[43]
Graphene (15.0wt%)	50.5	2480	6.38	3.21	6.82×10^{-5}	[4]
MnO ₂ (5.0wt%)	849.45	1.88×10^{-4}	1.36×10^{-4}	0.72	7.59×10^{-7}	[75]
Graphene (15wt%)	34	1620	–	–	0.44×10^{-3}	[41]
CNT (5.0wt%)	–66	22	0.12	–	0.38×10^{-4}	[32]
Graphene (0.15%)	1859.23	0.21×10^{-2}	6.55×10^{-2}	–	–	[50]

Table 2. Table from Ghosh et al. (2019) comparing the Seebeck coefficient due to various carbon-based materials and metallic oxides mixed with cement. The material that produced the highest coefficient is ZnO, followed by Fe₂O₃.

Table 1

Summary of thermoelectric properties for cement based composites with carbon and metallic oxide inclusions.

Materials	Preparation technique	Concentration (wt%)	Measurements				Ref.
			S ($\mu\text{V}/^\circ\text{C}$)	$\sigma (\text{Scm}^{-1})$	$\kappa (\text{Wm}^{-1}\text{K}^{-1})$	ZT	
Carbon fibers	Polyacrylonitrile	2.0	5.5	0.01	–	–	[11]
Carbon fibers and silica fume	Intercalation	1.0 and 15.0	-17.0	–	–	–	[12]
Expanded graphite	–	15.0	-54.5	24.8	3.213	6.82×10^{-4} at 75°C	[13]
Steel fibers	–	2.5	-31.0	7.14×10^{-4}	–	–	[14]
Steel slag-carbon fibers	–	–	14.4	–	–	–	[15]
Carbon nanotubes	–	15.0	57.98	0.818	0.947	9.33×10^{-5} at 75°C	[16]
Steel fibers	–	1.0	68.5	3.13×10^{-5}	–	–	[17]
Carbon fiber mineral admixtures	–	–	127.4	–	–	–	[18]
Carbon fibers	Pyrolytic carbon layer	5.0	–	2×10^{-5}	0.22	3.11×10^{-3} at 55.5°C	[19]
Carbon fibers and $\text{Ca}_3\text{Co}_4\text{O}_9$	–	1.0 and 3.0	58.6	–	–	–	[20]
Fe_2O_3	–	5.0	2500	1.5×10^{-8}	–	–	[21]
ZnO	–	5.0	3300	1.7×10^{-8}	–	–	[21]
MnO_2	–	–	-5490	–	–	–	[22]

Table 3. A table found in Ran et al. (2024) that describes the various mechanical properties of a variety of mechanical samples. The names of each of the mixes are shown in an M-V-X format representing the percent volume (V) and length in mm (X). This demonstrates that in addition to increasing thermoelectric electricity, carbon fibers also can increase the strength of cement.

Mix	Density (kg/m^3)	Compressive strength (MPa)	Tensile first crack stress (MPa)	Tensile strength (MPa)	Tensile strain capacity (%)
Control	1146 (5.7)	27.1 (1.3)	2.3 (0.38)	4.75 (0.20)	8.1 (0.31)
M-0.5-1	1003 (18.1)	23.8 (0.2)	3.02 (0.16)	4.34 (0.27)	10.67 (0.49)
M-1.0-1	1041 (7.3)	27.8 (1.1)	3.01 (0.01)	4.00 (0.04)	5.08 (0.42)
M-0.5-3	1028 (6.1)	25.2 (2.2)	3.02 (0.07)	3.91 (0.28)	4.93 (1.76)
M-1.0-3	1132 (13.1)	31.1 (3.6)	3.07 (0.49)	4.32 (0.56)	4.15 (1.59)
M-0.5-6	1111 (2.4)	30.4 (1.9)	2.99 (0.18)	4.23 (0.18)	5.67 (2.26)
M-1.0-6	1120 (6.4)	32.2 (1.3)	3.45 (0.09)	4.49 (0.19)	1.78 (0.17)
M-0.5-9	1131 (23.3)	33.4 (3.2)	4.03 (0.02)	5.83 (0.81)	6.43 (0.68)
M-1.0-9	1152 (29.4)	36.8 (2.8)	3.81 (0.52)	5.13 (0.49)	4.68 (0.75)
M-0.5-12	1126 (16.8)	30.3 (1.6)	3.07 (0.06)	5.04 (0.27)	7.89 (0.59)
M-1.0-12	1157 (46.1)	32.0 (0.3)	3.99 (0.52)	5.03 (0.47)	2.71 (0.37)
M-0.5-15	1082 (42.7)	30.2 (0.2)	3.03 (0.42)	4.58 (0.79)	4.51 (1.98)
M-1.0-15	1143 (17.1)	31.9 (0.8)	3.31 (0.31)	4.23 (0.14)	3.54 (0.61)
M-0.5-20	1151 (28.2)	31.2 (2.4)	3.15 (0.34)	4.05 (0.46)	3.32 (0.82)
M-1.0-20	1138 (38.2)	32.4 (1.5)	3.27 (0.40)	4.54 (0.56)	4.61 (1.37)

References

- Ghosh, S., Harish, S., Rocky, K. A., Ohtaki, M., & Saha, B. B. (2019). Graphene enhanced thermoelectric properties of cement based composites for building energy harvesting. *Energy and Buildings*, 202, 109419. <https://doi.org/10.1016/j.enbuild.2019.109419>
- Hai Yong Cao, Yao, W., & Jun Jie Qin. (2010). Seebeck Effect in Graphite-Carbon Fiber Cement Based Composite. *Advanced Materials Research*, 177, 566–569. <https://doi.org/10.4028/www.scientific.net/amr.177.566>
- Jaziri, N., Boughamoura, A., Müller, J., Mezghani, B., Tounsi, F., & Ismail, M. (2019). A comprehensive review of Thermoelectric Generators: Technologies and common applications. *Energy Reports*, 6. <https://doi.org/10.1016/j.egyr.2019.12.011>
- Ji, T., Zhang, S., He, Y., Zhang, X., & Li, W. (2022). Enhanced Thermoelectric Efficiency of Cement-Based Materials with Cuprous Oxide for Sustainable Buildings. *Advances in Materials Science and Engineering*, 2022, 1–11. <https://doi.org/10.1155/2022/6403756>
- Li, W., Du, C., Liang, L., & Chen, G. (2025). Cement-Based Thermoelectric Materials, Devices and Applications. *Nano-Micro Letters*, 18(1). <https://doi.org/10.1007/s40820-025-01866-2>
- NASA. (2023, June 13). *Power: Radioisotope Thermoelectric Generators*. Science.nasa.gov. <https://science.nasa.gov/planetary-science/programs/radioisotope-power-systems/power-radioisotope-thermoelectric-generators/>
- Piao, R., Woo, S. Y., Lee, D., Jeong, C. K., Banthia, N., & Yoo, D.-Y. (2025). Investigating the effect of carbon fiber dosage on the mechanical and thermoelectric properties of ultra-high-performance fiber-reinforced concrete. *Journal of Sustainable Cement-Based Materials*, 14(9), 1937–1951. <https://doi.org/10.1080/21650373.2025.2511767>

Ran, H., Elchalakani, M., Ali Sadakkathulla, M., Yehia, S., Cai, J., & Xie, T. (2024).

Thermoelectric engineered cementitious composites with low thermal conductivity for efficiency improvement of buildings. *Energy and Buildings*, 317, 114390.

<https://doi.org/10.1016/j.enbuild.2024.114390>

Reardon, C. (2020). *Thermal Mass*. Your Home; Australian Government.

<https://www.yourhome.gov.au/passive-design/thermal-mass>

Singh, V. P., Kumar, M., Srivastava, R. S., & Vaish, R. (2021). Thermoelectric energy harvesting using cement-based composites: a review. *Materials Today Energy*, 21, 100714.

<https://doi.org/10.1016/j.mtener.2021.100714>

Tong, S., Prior, J., McGregor, G., Shi, X., & Kinney, P. (2021). Urban heat: An increasing threat to global health. *The BMJ*, 375(2467). <https://doi.org/10.1136/bmj.n2467>

US EPA. (2024, August 2). *Learn About Heat Island Effects* | US EPA. US EPA.

<https://www.epa.gov/heatislands/learn-about-heat-island-effects>

Wan, Y., Tan, S., Li, L., Zhou, H., Zhao, L., Li, H., & Han, Z. (2023). Fabrication and thermoelectric property of the nano Fe₂O₃/carbon fiber/cement-based composites for potential energy harvesting application. *Construction and Building Materials*, 365, 130021–130021. <https://doi.org/10.1016/j.conbuildmat.2022.130021>

Wei, J.-J., Zhang, Q., Zhao, L., Hao, L., & Nie Zhengbo. (2017). Effect of moisture on the thermoelectric properties in expanded graphite/carbon fiber cement composites. *Ceramics International*, 43(14), 10763–10769.

<https://doi.org/10.1016/j.ceramint.2017.05.088>

Wei, T.-R., Guan, M., Yu, J., Zhu, T., Chen, L., & Shi, X. (2018). How to Measure Thermoelectric Properties Reliably. *Joule*, 2(11), 2183–2188.

<https://doi.org/10.1016/j.joule.2018.10.020>

Zafra, M. (2025, July 1). The Floor Is Lava. *Reuters*.

<https://www.reuters.com/graphics/CLIMATE-CHANGE/URBAN-HEAT/byvrejywdpe/>